

Likelihood Non-Gaussianity in Large Scale Structure Analyses

ChangHoon Hahn, et al.

Lawrence Berkeley National Laboratory, 1 Cyclotron Rd, Berkeley CA 94720, USA

changhoon.hahn@lbl.gov

DRAFT --- d0b499c --- 2017-12-08 --- NOT READY FOR DISTRIBUTION

ABSTRACT

abstract here

Subject headings: methods: statistical — galaxies: statistics — methods: data analysis — cosmological parameters — cosmology: observations — large-scale structure of universe

1. Introduction

- Talk about the use of Bayesian parameter inference and getting the posterior in LSS cosmology
- Explain the two major assumptions that go into evaluating the likelihood
- Emphasize that we are not talking about non-Gaussian contributions to the likelihood
- Emphasize the scope of this paper is to address whether one of the assumptions matters for galaxy clustering analyses.

2. Gaussian Likelihood Assumption

- Depending on Hogg’s paper maybe a simple illustration of how the likelihood assumption

However, as we show in this paper, the assumption of likelihood Gaussianity is not necessary. In fact, we will show that the mock catalogs used in standard LSS analyses to estimate the covariance matrix for evaluating the Gaussian likelihood, can be used to quantify the non-Gaussianity. More important the mock catalogs can be used to construct an accurate estimator for the non-Gaussian likelihood.

3. Mock Catalogs

Mock catalogs are play an indispensable role in standard cosmological anlsyses of LSS studies. They’re used for testing analysis pipelines (Beutler et al. 2017; Grieb et al. 2017; Tinker & et al. in preparation), testing the effect of systematics (Guo et al. 2012; Vargas-Magaña et al. 2014; Hahn et al. 2017; Pinol et al. 2017; Ross et al. 2017), and, most relevantly for this paper, estimating the covariance matrix (Parkinson et al. 2012; Kazin et al. 2014; Grieb et al. 2017; Alam et al. 2017; Beutler et al. 2017; Sinha et al. 2017). In fact, nearly all current state-of-the-art LSS analyses use covariance matrices estimated from mocks to evaluate the likelihood for parameter inference.

While some argue for analytic estimates of the covariance matrix (e.g. Mohammed et al. 2017) or estimates directly from data by subsampling (e.g. Norberg et al. 2009), covariance matrices from mocks have a number of advantages. Mock catalogs allow us to incorporate detailed systematic errors present in the data and variance beyond the volume of the data. Even for analytic estimates, large ensembles of mocks are crucial for validataion (Slepian et al. 2017). Moreover, as we show later in this paper, mock catalogs present an additional advantage: they allow us to quantify the non-Gaussianity of the likelihood and more accurately estimate the true likelihood.

In this paper, we we focus on two LSS analyses: the powerspectrum multipole full shape analysis of Beutler et al. (2017) and group multiplicity function analysis of Sinha et al. (2017). Throughout the paper we will make extensive use of the mock catalogs used in these analyses. In this section, we give a brief description of these mocks and how the observables used in the analysis – the powerspectrum multipole (P_ℓ) and group multiplicity function ($\zeta(N)$) – are calculated from them. Afterwards, we will describe how we compute the covariance matrix, \mathbb{C} , and the pre-processed mock observable date, \mathbf{X}^{mock} .

3.1. MultiDark-PATCHY Mock Catalog

In their powerspectrum multipole full shape analysis, Beutler et al. (2017) use the MultiDark-PATCHY mock catalogs from Kitaura et al. (2016). These mocks are generated using the PATCHY code (Kitaura et al. 2014, 2015). They rely on large-scale density fields generated using augmented Lagrangian Perturbation Theory (ALPT; Kitaura & Heß 2013) on a mesh. This mesh is then populated with galaxies based on a combined non-linear deterministic and stochastic biases. The mocks from the PATCHYcode are then calibrated to reproduce the galaxy clustering in the high-fidelity BigMultiDark N -body simulation (Rodríguez-Torres et al. 2016; Klypin et al. 2016).

The galaxies are then assigned stellar masses using the HADRON code (Zhao et al. 2015). And the SUGAR code (Rodríguez-Torres et al. 2016) is applied to combine different boxes, incorporate selection effects and masking to produce mock light-cone galaxy catalogs. The

statistics of the resulting mocks are then compared to observations and the process is iterated to reach desired accuracy. We refer readers to [Kitaura et al. \(2016\)](#) for further details.

In total, [Kitaura et al. \(2016\)](#) generated a 12,228 mock light-cone galaxy catalogs for BOSS Data Release 12: 2048 for each southern and northern galactic caps of LOWZ, CMASS, combined samples. In [Beutler et al. \(2017\)](#), they use 2045 and 2048 for the northern galactic cap (NGC) and southern galactic cap (SGC) of the LOWZ+CMASS combined sample. [Beutler et al. \(2017\)](#) excluded 3 mock realizations, due to notable issues, which have been since been addressed. Therefore, in our analysis we use all 2048 mocks for both the NGC and SGC of the LOWZ+CMASS combined sample.

3.2. [Sinha et al. \(2017\)](#) Mocks

The simulations used in the small-scale clustering analysis of [Sinha et al. \(2017\)](#) are from the Large Suite of Dark Matter Simulations project (LasDamas; [McBride et al. 2009](#)). More specifically [Sinha et al. \(2017\)](#) uses the Consuelo and Carmen configurations, which were designed to model SDSS galaxies with M_r thresholds of -19 and -21 , respectively. The initial conditions for these simulations are derived from second order Lagrangian Perturbation Theory using the 2LTPIC code ([Scoccimarro 1998](#); [Crocce et al. 2006](#)) and evolved using the N -body GADGET – 2 code ([Springel 2005](#)). Halos are then identified from the dark matter distribution outputs using the `ntropy – fofsv` code ([Gardner et al. 2007](#)), which uses a friend-of-friends algorithm (FoF; [Davis et al. 1985](#)) with a linking length of 0.2 times the mean inter-particle separation. The FoF halo masses are then adjusted using the [Warren et al. \(2006\)](#) correction. The Consuelo simulation contains 1400^3 dark matter particles with mass of $1.87 \times 10^9 h^{-1} M_\odot$ in a cubic volume of $420 h^{-1} Mpc$ per side and is evolved from $z_{\text{init}} = 99$. The Carmen simulation contains 1120^3 dark matter particles with mass of $4.938 \times 10^{10} h^{-1} M_\odot$ in a cubic volume of $1000 h^{-1} Mpc$ per side and is evolved from $z_{\text{init}} = 49$. They use the following cosmological parameters, which are motivated by the WMAP3 constraints ([Spergel et al. 2007](#)): $\Omega_m = 0.25$, $\Omega_\Lambda = 0.75$, $\Omega_b = 0.04$, $h = 0.7$, $\sigma_8 = 0.8$, and $n_s = 1.0$.

The FoF halo catalogs are then populated with galaxies using the ‘Halo Occupation Distribution’ (HOD) framework. In this framework, the number, positions, and velocities of galaxies are described statistically by an HOD model. [Sinha et al. \(2017\)](#) adopts the ‘vanilla’ HOD model of [Zheng et al. \(2007\)](#), where the mean number of central and satellite galaxies are described by the halo mass and five HOD parameters: M_{min} , $\sigma_{\log M}$, M_0 , M_1 , and α . Finally, once the simulation boxes are populated with galaxies, observational systematic effects are imposed. The peculiar velocities of galaxies are used to impose redshift-space distortions. And galaxies that lie outside the redshift limits or sky footprint of the SDSS sample are removed. For further details regarding the LasDamas simulations or mock catalogs, we refer readers to [Sinha et al. \(2017\)](#).

To calculate their covariance matrix, [Sinha et al. \(2017\)](#) produced 200 independent mock

catalogs from 50 simulations using a single set of HOD model parameters. To take advantage of the methods we present in this work (Sections [ref](#)), we require a large number of mock catalogs. Our methods rely on sampling multidimensional distributions, so incorporating more mocks into the analysis drastically improves their accuracy. Therefore, we utilize an additional 19,800 mock catalogs made from the procedure. These mocks are not generated using the same set of HOD model parameters, but 200 mocks each from 99 sets of HOD parameters sampled from the MCMC chain used to produce the posterior probability distribution presented in [Sinha et al. \(2017\)](#).

3.3. Mock Observable \mathbf{X}^{mock} and Covariance Matrix \mathbb{C}

In [Beutler et al. \(2017\)](#) and [Sinha et al. \(2017\)](#) they analyze the powerspectrum multipoles measured from the BOSS DR12 galaxies and the group multiplicity function measured from the SDSS DR7 galaxies, respectively. To get from the mock catalogs described above to the covariance matrices used in these analyses, the observables must be consistently measured for each mock catalog. Below we briefly describe how $P_\ell(k)$ and $\zeta(N)$ and their covariance matrices are measured in [Beutler et al. \(2017\)](#) and [Sinha et al. \(2017\)](#). Furthermore, we describe how we pre-process the mock observables to be used in the methods we describe in the next sections.

To measure the powerspectrum multipoles of the BOSS DR12 galaxies and the MutliDark-PATCHY mocks (Section 3.1), [Beutler et al. \(2017\)](#) uses a fast fourier transform (FFT) based anisotropic powerspectrum estimator based on [Bianchi et al. \(2015\)](#) and [Scoccimarro \(2015\)](#). This estimator estimates the monopole, quadrupole, and hexadecapole ($\ell = 0, 2$, and 4) of the powerspectrum using FFTs of the overdensity field multipoles for a given survey geometry. By using FFTs rather than counting all galaxy pairs, the estimator significantly reduces the computational costs to $\mathcal{O}(N \log N)$, where N is the number of grid cells used to bin the galaxy data. The powerspectrum multipoles are calculated in bins of $\Delta k = 0.01 h\text{Mpc}^{-1}$. The powerspectrum monopole and quadrupole are computed over the range $k = 0.01 - 0.15 h\text{Mpc}^{-1}$ while the hexadecapole is computed over the range $k = 0.01 - 0.10 h\text{Mpc}^{-1}$. For further details on the estimator we refer readers to Section 3 of [Beutler et al. \(2017\)](#).

Using the $P_\ell(k)$ of the MultiDark-PATCHY mocks, [Beutler et al. \(2017\)](#) then computes the covariance matrix of all multipoles as

$$\mathbb{C}_{xy} = \frac{1}{N_{\text{mock}} - 1} \sum_{n=1}^{N_{\text{mock}}} [P_{\ell,n}(k_i) - \bar{P}_\ell(k_i)] \times [P_{\ell',n}(k_j) - \bar{P}_{\ell'}(k_j)]. \quad (1)$$

N_{mock} is the number of mock catalogs and \bar{P}_ℓ is the mean of the mock powerspectra:

$$\bar{P}_\ell(k_i) = \frac{1}{N_{\text{mock}}} \sum_{n=1}^{N_{\text{mock}}} P_{\ell,n}(k_i). \quad (2)$$

The (x, y) element of \mathbb{C} is given by $(x, y) = (n_b \frac{\ell}{2} + i, n_b \frac{\ell'}{2} + j)$, where n_b is the number of bins in each multipole power spectrum ($n_b = 14$ for the monopole and quadrupole; $n_b = 9$ for the hexadecapole). \mathbb{C} is a 37×37 matrix.

In this work, we compute the $P_\ell(k)$ of the MultiDark-PATCHY mocks, using a similar FFT-based estimator of [Hand et al. \(2017\)](#) instead of the estimator in [Beutler et al. \(2017\)](#). Our choice was based on computational convenience. A python implementation of the [Hand et al. \(2017\)](#) estimator is publicly available in the NBODYKIT package³. We emphasize that the resulting $P_\ell(k)$ s and covariance matrix from the two estimators have been confirmed to be consistent with one another.

Next, for the [Sinha et al. \(2017\)](#) group multiplicity function analysis, they start with the [Berlind et al. \(2006\)](#) friend-of-friend algorithm to identify groups in the SDSS and mock data. According to the algorithm, a galaxy pair is assigned to the same group if their projected and line-of-sight separations are both less than the corresponding linking length. [Sinha et al. \(2017\)](#) adopts the [Berlind et al. \(2006\)](#) linking lengths: $b_\perp = 0.14$ and $b_\parallel = 0.75$. These linking lengths are in units of mean inter-galaxy separation $n_g^{-1/3}$, where n_g is the number density of the sample. In comoving lengths, the linking lengths for the SDSS DR7 $M_r < -19$ sample correspond to $(r_\perp, r_\parallel) = (0.57, 3.05)h^{-1}\text{Mpc}$. Once the groups are identified in the SDSS and mock data, $\zeta(N)$ is derived by calculating the comoving number density of groups in bins of richness N – the number of galaxies in the group. For the $M_r < 19$ SDSS sample, [Sinha et al. \(2017\)](#) uses eight N bins: $(5 - 6)$, $(7 - 9)$, $(10 - 13)$, $(14 - 19)$, $(20 - 32)$, $(33 - 52)$, $(53 - 84)$, $(85 - 220)$. For further details on the GMF calculation, we refer readers to Section 4.2 of [Sinha et al. \(2017\)](#).

From the GMFs of each mocks, [Sinha et al. \(2017\)](#) computes the covariance matrix for the analysis as

$$\mathbb{C}_{ij} = \frac{1}{N_{\text{mock}} - 1} \sum_{n=1}^{N_{\text{mock}}} [\zeta_n(N_i) - \bar{\zeta}(N_i)] \times [\zeta_n(N_j) - \bar{\zeta}(N_j)]. \quad (3)$$

In [Sinha et al. \(2017\)](#), they compute the covariance matrix using 200 mocks generated using a single fiducial set of HOD parameters. However, as we mention in Section 3.2, in this paper we use 20,000 mocks from 100 different set of HOD parameters sampled from the MCMC chain. Consistent with this, the GMF covariance matrix we use in this paper is computed as Eq. 3 but with the $N_{\text{mock}} = 20,000$ mocks.

In the rest of this paper we investigate the non-Gaussianity of the likelihood and its impact on parameter inference for both [Beutler et al. \(2017\)](#) and [Sinha et al. \(2017\)](#). In order to discuss the two separate analyses in a consistent manner, we define the matrix \mathbf{D}^{mock} of the

³<http://nbodykit.readthedocs.io/en/latest/index.html>

mock observables (P_ℓ and ζ) as follows.

$$\mathbf{D}^{\text{mock}} = \{\mathbf{D}_n^{\text{mock}}\} \quad (4)$$

where $\mathbf{D}_n^{\text{mock}} = [P_0(k)_n, P_2(k)_n, P_4(k)_n]$ for Beutler et al. (2017) and $\mathbf{D}_n^{\text{mock}} = \zeta(N)_n$ for Sinha et al. (2017). The \mathbf{D}^{mock} matrix has dimensions of $N_{\text{mock}} \times N_{\text{bin}}$, where N_{bin} is the number of bins in the observable. For B2017, $N_{\text{mock}} = 2048$ and $N_{\text{bin}} = 37$. Meanwhile, for S2017, $N_{\text{mock}} = 20,000$ and $N_{\text{bin}} = 8$.

For the methods we later describe in Section [ref](#), the mock observable data (\mathbf{D}^{mock}) need to be pre-processed. This pre-processing involves two steps: mean-subtraction and whitening. For mean subtraction, the mean of the observable, $\bar{\mathbf{D}}^{\text{mock}} = \bar{P}_\ell$ or $\bar{\zeta}$, is subtracted from \mathbf{D}^{mock} . Then $\mathbf{D}^{\text{mock}} - \bar{\mathbf{D}}^{\text{mock}}$ is whitened using a linear transformation to remove the Gaussian correlation between the bins of \mathbf{D}^{mock} :

$$\mathbf{X}^{\text{mock}} = L (\mathbf{D}^{\text{mock}} - \bar{\mathbf{D}}^{\text{mock}}). \quad (5)$$

The linear transformation is derived so that covariance matrix of the whitened data, \mathbf{X}^{mock} , is the identity matrix \mathbb{I} . Such a whitening linear transformation can be derived in infinite ways. One way to derive the linear transformation is through the eigen-decomposition of the covariance matrix (*e.g.* Hartlap et al. 2009; Sellentin et al. 2017). We, alternatively, derive the linear transformation \mathbf{L} using Cholesky decomposition of the inverse covariance matrix (?): $\mathbb{C}^{-1} = \mathbf{L} \mathbf{L}^T$. **We confirm tha the different whitening algorithms, does not impact the results of the paper.** Now that we have the pre-processed data of the mock observables, we proceed in the next section to quantifying the non-Gaussianity of the P_ℓ and ζ likelihoods using \mathbf{X}^{mock} .

4. Quantifying the Likelihood non-Gaussianity

The standard approach to parameter inference in LSS studies neglects to account for likelihood non-Gaussianity (Section 2). However, we are not the first to investigate likelihood non-Gaussianity in LSS analyses. Nearly two decades ago, Scoccimarro (2000) examined the likelihood non-Gaussianity for the powerspectrum and reduced bispectrum using mock catalogs of the IRAS redshift catalogs. More recently, Hartlap et al. (2009) and Sellentin et al. (2017) examined the non-Gaussianity of the cosmic shear correlation function likelihood using simulations of the Chandra Deep Field South and CFHTLenS, respectively.

While these works present different methods for identifying likelihood non-Gaussianity, they do not present a concrete way of quantifying it. For instance, Hartlap et al. (2009) identifies the non-Gaussianity of the cosmic shear likelihood by looking at the statistical independence/dependence of PCA components of the mock observable datavector. In Sellentin et al. (2017), they use the Mean Integrated Squared Error (MISE) as a distance metric between Gaussian random variables and the whitened mock observable datavector to identify

non-Gaussian correlations between two elements of the data vector. These indirect measures of likelihood non-Gaussianity are challenging to interpret and extend more generally to LSS studies.

A more direct approach, however, can be taken to quantify the non-Gaussianity of the likelihood. We can calculate the divergence between the distribution of our observable, $p(x)$, and $q(x)$ a multivariate Gaussian described by the average of the mocks and the covariance matrix. The following are two of the most commonly used divergences: the Kullback-Leibler (hereafter KL) divergence

$$D_{KL}(p \parallel q) = \int p(x) \log \frac{p(x)}{q(x)} dx \quad (6)$$

and the Rényi- α divergence

$$D_{R-\alpha}(p \parallel q) = \frac{1}{\alpha - 1} \log \int p^\alpha(x) q^{1-\alpha}(x) dx. \quad (7)$$

In the limit as α approaches 1, the Rényi- α divergence is equivalent to the KL divergence.

Of course, in our case, we don't know $p(x)$ — *i.e.* the distribution of our observable. If we did, we would simply use that instead of bothering with the covariance matrix or this paper. We can, however, still estimate the divergence using nonparametric divergence estimators (Wang et al. 2009; Póczos et al. 2012; Krishnamurthy et al. 2014). These estimators, allows us to estimate the divergence directly from samples $X_{1:n} = \{X_1, \dots, X_n\}$ and $Y_{1:m} = \{Y_1, \dots, Y_m\}$ drawn from p and q respectively: $\hat{D}_\alpha(X_{1:n} \parallel Y_{1:m})$.

For instance, the estimator presented in Póczos et al. (2012) allows us to estimate the kernel function of the Rényi- α divergence,

$$D_\alpha(p \parallel q) = \int p^\alpha(x) q^{1-\alpha}(x) dx. \quad (8)$$

using k th nearest neighbor density estimators. Let $\rho_k(x)$ denote the Euclidean distance of the k th nearest neighbor of x in the sample $X_{1:n}$ and $\nu_k(x)$ denote the Euclidean distance of the k th nearest neighbor of x in the sample $Y_{1:m}$. Then $D_\alpha(p \parallel q)$ can be estimated as

$$\hat{D}_\alpha(X_{1:n} \parallel Y_{1:m}) = \frac{B_{k,\alpha}}{n} \left(\frac{n-1}{m} \right)^{1-\alpha} \sum_{i=1}^n \left(\frac{\rho_k^d(X_i)}{\nu_k^d(X_i)} \right)^{1-\alpha}, \quad (9)$$

where $B_{k,\alpha} = \frac{\Gamma(k)^2}{\Gamma(k-\alpha+1)\Gamma(k+\alpha-1)}$. Póczos et al. (2012) goes to further prove that this estimated kernel function is asymptotically unbiased,

$$\lim_{n,m \rightarrow \infty} \mathbb{E}[\hat{D}_\alpha(X_{1:n} \parallel Y_{1:m})] = D_\alpha(p \parallel q). \quad (10)$$

Plugging $\hat{D}_\alpha(X_{1:n} \parallel Y_{1:m})$ into Eq. 7, we get an estimator for the Rényi- α divergence. A similar estimator (Wang et al. 2009) can also be derived for the KL divergence (Eq. 6). We note that while the divergence estimators converge to the true divergence with a large enough samples, with a limited number of samples from the distribution, the estimators are noisy.

These divergence estimates have been applied to Support Vector Machines and used extensively in the machine learning and astronomical literature with great success **elaborate a lot more**

- Compile papers that use this divergence, Ntampaka et al. (2015, 2016)

For more details on the non-parametric divergence estimators, we refer readers to Póczos et al. (2012) and Krishnamurthy et al. (2014).

Now we can use the divergence estimators above to quantify the non-Gaussianity of the likelihood. In other words, we’re intersted in the divergence between the distribution $p(x)$ sampled by the mock observables \mathbf{X}^{mock} (Section 3.3) and the multivariate Gaussian “pseudo-likelihood” distribution assumed in standard analyses – $\mathcal{N}(\bar{\mathbf{X}}^{\text{mock}}, \mathbb{C})$. Since \mathbf{X}^{mock} is a sample from $p(x)$, we draw a reference sample \mathbf{Y}^{ref} from $\mathcal{N}(\bar{\mathbf{X}}^{\text{mock}}, \mathbb{C})$ to use in the estimators. Similar to the experiments detailed in Póczos et al. (2012), we construct \mathbf{Y}^{ref} with a comparable sample size as \mathbf{X}^{mock} : 2000 and 10,000 for the P_ℓ and ζ analyses respectively. In Figure 2, we compare the distribution of Rényi- α (left) and KL (right) divergence estimates (orange) $\hat{D}_{R\alpha}$ and \hat{D}_{KL} between the mock data \mathbf{X}^{mock} and a reference sample \mathbf{Y}^{ref} for the $P_\ell(k)$ (top) and $\zeta(N)$ (bottom) analyses. These distributions were constructed using **100** divergence estimates, where \mathbf{Y}^{ref} is resampled for each estimate. In order to illustrate the scatter of the estimators and also as a reference point for the comparison, we include (blue) the distribution of $\hat{D}_{R\alpha}(\mathbf{X}^{\text{ref}} \parallel \mathbf{Y}^{\text{ref}})$ and $\hat{D}_{KL}(\mathbf{X}^{\text{ref}} \parallel \mathbf{Y}^{\text{ref}})$ where \mathbf{X}^{ref} is a data vector with the same dimension as \mathbf{X}^{mock} sampled from $\mathcal{N}(\bar{\mathbf{X}}^{\text{mock}}, \mathbb{C})$.

The discrepancy between the blue and orange distributions illustrates the non-Gaussianity of $p(x)$ sampled by \mathbf{X}^{mock} .

- Describe the discrepancy.

5. Estimating the Non-Gaussian Likelihood

In the previous section, we estimate the divergence between the P_ℓ and ζ likelihoods sampled by mocks and their respective Gaussian pseudo-likelihoods. The divergence estimates quantify the non-Gaussianity of the likelihoods and **discredit** the Gaussian likelihood assumption in standard LSS studies. Our ultimate goal, however, goes beyond demonstrating this non-Gaussianity. We’re interested in quantifying the impact of likelihood non-Gaussianity on the final cosmological parameter constraints and also in developing more

accurate methods for parameter inference in LSS analyses.

While the divergence estimates of the previous are useful for quantifying non-Gaussianity, it’s not clear how they propagate onto the inferred parameter constraints. In this section, we present two methods for estimating the non-Gaussian likelihood distribution of P_ℓ and ζ from the corresponding mocks. These methods will be used later to quantify the impact of likelihood non-Gaussianity on the parameter constraints of B2017 and S2017. Moreover, they provide a general framework for more accurately estimating the likelihood distribution than the Gaussian pseudo-likelihood.

5.1. Gaussian Mixture Likelihood Estimation

When mock catalogs are used in LSS analyses to estimate the covariance matrix, they are used as data points sampling the likelihood distribution. When constructing the pseudo-likelihood, this distribution is assumed to have a Gaussian functional form. However, the Gaussian functional form, or any functional form for that matter, is not necessary to estimate the likelihood distribution. Instead the N_{bin} -dimensional likelihood distribution can be directly estimated from the set of mock catalogs using – for instance, Gaussian mixture density estimation.

Gaussian mixture density estimation is a “semi-parametric” method that uses a Gaussian mixture model, a weighted sum of k Gaussian component densities

$$p(\mathbf{x}) = \sum_{i=1}^k \pi_i \mathcal{N}(\mathbf{x}; \boldsymbol{\theta}_i), \quad (11)$$

to estimate the density (?). The component weights (π_i ; also known as mixing weights) and the component parameters $\boldsymbol{\theta}_i$ are free parameters of the mixture model. Most popularly, the free parameter of the model are estimated through an expectation-maximization (EM) algorithm (Dempster et al. 1977). The EM algorithm initiates by randomly assigning $\boldsymbol{\theta}_i^0$ to the k Gaussian componenets. The algorithm then iterates between two steps. In the first step, the algorithm computes, for each point, a probability of being generated by each component of the model. These probabilities can be thought of as probabilistic assignments of the points to the components. Next, given the assignment of the data points to the components, $\boldsymbol{\theta}_i^t$ of each component are updated to $\boldsymbol{\theta}_i^{t+1}$ to maximize the likelihood of the assigned points. This process is repeated until convergence *i.e.* when the log-likelihood of the data given the mixture model converges.

More commonly, rather than using randomly assigned initial $\boldsymbol{\theta}_i$

More specific choices we make in our GMM algorithm

- k means initial conditions

Bayesian Information Criteria to determine k

talk about how this is used extensively in ML and even astronomy (see also references in Kuhn & Feigelson 2017) This direct approach is particularly promising for the case of S2017, where we have $N_{\text{mock}} = 20,000$ samples of an $N_{\text{bin}} = 8$ dimensional distribution. As an illustration of Gaussian mixture density estimation, in Figure we show Gaussian mixture models of the highest N bin of \mathbf{X}^{mock} .

5.2. Independent Component Analysis

Curse of dimensionality! 2048 mocks in Beutler not enough to directly estimate the 37-dimensional space, so we use independent component analysis Hartlap et al. (2009)

- equation
- Similar figure to Hartlap et al. (2009) that tests the independence?
- Kernel Density Estimation
-

Figure 2

6. Impact on Parameter Inference

6.1. MCMC

- details of each of the MCMC runs

6.2. Importance Sampling

- equations explaining importance sampling framework

Figure 3

Figure 4

7. Discussion

- Will it matter for future surveys?
- Likelihood free inference (cite justin's paper)

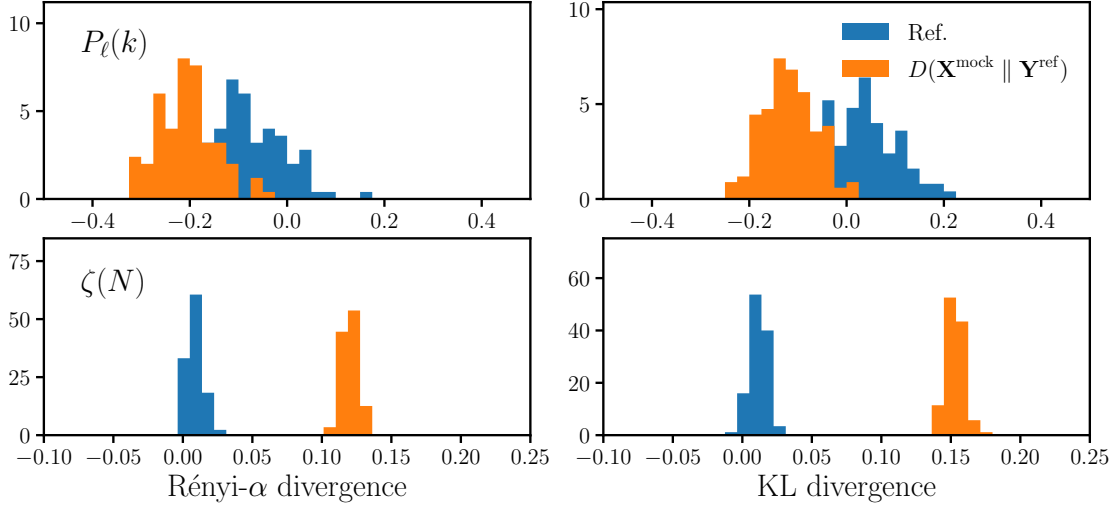


Fig. 1.— Rényi- α and KL divergence estimates, ($D_{R\alpha}$ and D_{KL}), between the mock data \mathbf{X}^{mock} and a reference sample \mathbf{Y}^{ref} for the $P_\ell(k)$ (left) and $\zeta(N)$ (right) analyses.

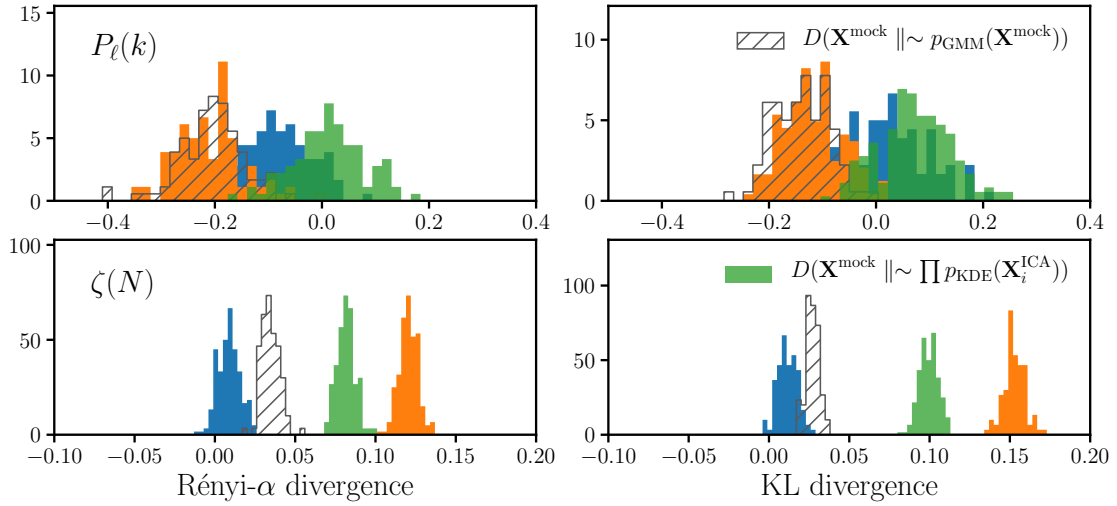


Fig. 2.—

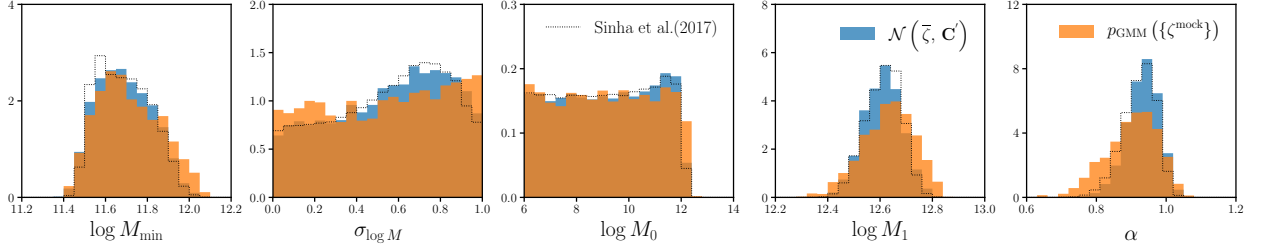


Fig. 3.—

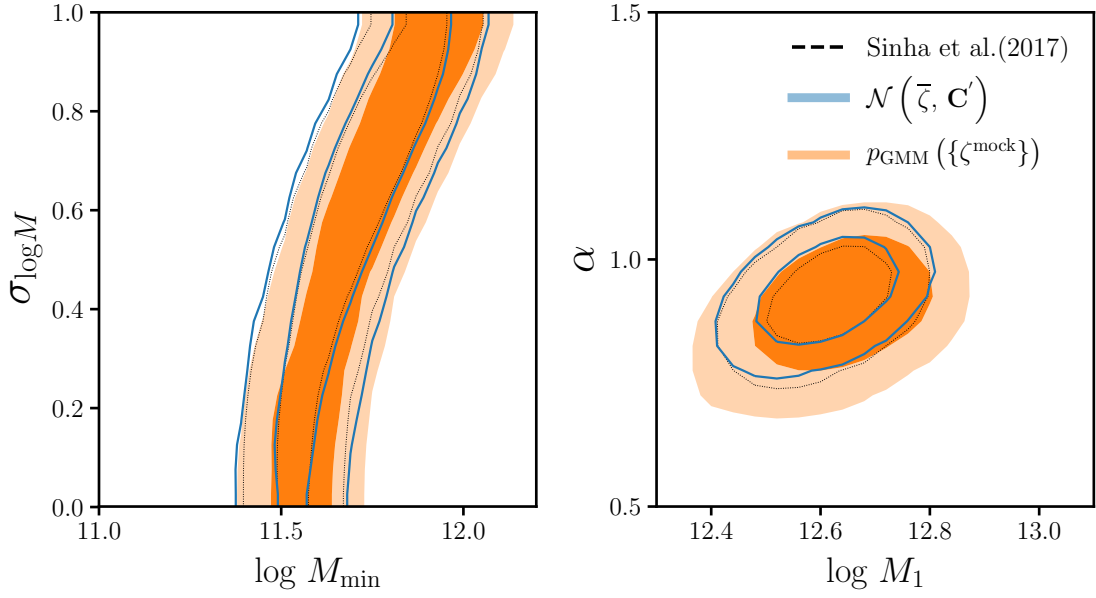


Fig. 4.—

8. Summary

Acknowledgements

It’s a pleasure to thank Simone Ferraro, David W. Hogg, Emmaneul Schaan, Roman Scoccimarro Zachary Slepian

REFERENCES

- Alam, S., Ata, M., Bailey, S., et al. 2017, [Monthly Notices of the Royal Astronomical Society](#), 470, 2617
- Berlind, A. A., Frieman, J., Weinberg, D. H., et al. 2006, [The Astrophysical Journal Supplement Series](#), 167, 1
- Beutler, F., Seo, H.-J., Saito, S., et al. 2017, [Monthly Notices of the Royal Astronomical Society](#), 466, 2242
- Bianchi, D., Gil-Marín, H., Ruggeri, R., & Percival, W. J. 2015, [Monthly Notices of the Royal Astronomical Society](#), 453, L11
- Crocce, M., Pueblas, S., & Scoccimarro, R. 2006, [Monthly Notices of the Royal Astronomical Society](#), 373, 369
- Davis, M., Efstathiou, G., Frenk, C. S., & White, S. D. M. 1985, [The Astrophysical Journal](#), 292, 371
- Dempster, A. P., Laird, N. M., & Rubin, D. B. 1977, *Journal of the Royal Statistical Society. Series B (Methodological)*, 39, 1
- Gardner, J. P., Connolly, A., & McBride, C. 2007, in *Astronomical Data Analysis Software and Systems XVI*, Vol. 376, 69
- Grieb, J. N., Sánchez, A. G., Salazar-Albornoz, S., et al. 2017, [Monthly Notices of the Royal Astronomical Society](#), 467, 2085
- Guo, H., Zehavi, I., & Zheng, Z. 2012, [The Astrophysical Journal](#), 756, 127
- Hahn, C., Scoccimarro, R., Blanton, M. R., Tinker, J. L., & Rodríguez-Torres, S. A. 2017, [Monthly Notices of the Royal Astronomical Society](#), 467, 1940
- Hand, N., Li, Y., Slepian, Z., & Seljak, U. 2017, [Journal of Cosmology and Astro-Particle Physics](#), 07, 002
- Hartlap, J., Schrabback, T., Simon, P., & Schneider, P. 2009, [Astronomy and Astrophysics](#), 504, 689
- Kazin, E. A., Koda, J., Blake, C., et al. 2014, [Monthly Notices of the Royal Astronomical Society](#), 441, 3524
- Kitaura, F.-S., Gil-Marín, H., Scóccola, C. G., et al. 2015, [Monthly Notices of the Royal Astronomical Society](#), 450, 1836
- Kitaura, F.-S., & Heß, S. 2013, [Monthly Notices of the Royal Astronomical Society](#), 435, L78

- Kitaura, F.-S., Yepes, G., & Prada, F. 2014, [Monthly Notices of the Royal Astronomical Society](#), **439**, L21
- Kitaura, F.-S., Rodríguez-Torres, S., Chuang, C.-H., et al. 2016, [Monthly Notices of the Royal Astronomical Society](#), **456**, 4156
- Klypin, A., Yepes, G., Gottlöber, S., Prada, F., & Heß, S. 2016, [Monthly Notices of the Royal Astronomical Society](#), **457**, 4340
- Krishnamurthy, A., Kandasamy, K., Poczos, B., & Wasserman, L. 2014, arXiv:1402.2966 [math, stat], [arXiv:1402.2966 \[math, stat\]](#)
- Kuhn, M. A., & Feigelson, E. D. 2017, arXiv:1711.11101 [astro-ph, stat], [arXiv:1711.11101 \[astro-ph, stat\]](#)
- McBride, C., Berlind, A., Scoccimarro, R., et al. 2009, in *Bulletin of the American Astronomical Society*, Vol. 213, 425.06
- Mohammed, I., Seljak, U., & Vlah, Z. 2017, [Monthly Notices of the Royal Astronomical Society](#), **466**, 780
- Norberg, P., Baugh, C. M., Gaztañaga, E., & Croton, D. J. 2009, [Monthly Notices of the Royal Astronomical Society](#), **396**, 19
- Ntampaka, M., Trac, H., Sutherland, D. J., et al. 2015, [The Astrophysical Journal](#), **803**, 50
—. 2016, [The Astrophysical Journal](#), **831**, 135
- Parkinson, D., Riemer-Sørensen, S., Blake, C., et al. 2012, [Physical Review D](#), **86**, 103518
- Pinol, L., Cahn, R. N., Hand, N., Seljak, U., & White, M. 2017, [Journal of Cosmology and Astroparticle Physics](#), **2017**, 008
- Póczos, B., Xiong, L., Sutherland, D. J., & Schneider, J. 2012, in [2012 IEEE Conference on Computer Vision and Pattern Recognition](#), 2989
- Rodríguez-Torres, S. A., Chuang, C.-H., Prada, F., et al. 2016, [Monthly Notices of the Royal Astronomical Society](#), **460**, 1173
- Ross, A. J., Beutler, F., Chuang, C.-H., et al. 2017, [Monthly Notices of the Royal Astronomical Society](#), **464**, 1168
- Scoccimarro, R. 1998, [Monthly Notices of the Royal Astronomical Society](#), **299**, 1097
—. 2000, [The Astrophysical Journal](#), **544**, 597
—. 2015, [Physical Review D](#), **92**, 083532
- Sellentin, E., Jaffe, A. H., & Heavens, A. F. 2017, arXiv:1709.03452 [astro-ph, stat], [arXiv:1709.03452 \[astro-ph, stat\]](#)
- Sinha, M., Berlind, A. A., McBride, C. K., et al. 2017, arXiv:1708.04892 [astro-ph], [arXiv:1708.04892 \[astro-ph\]](#)
- Slepian, Z., Eisenstein, D. J., Brownstein, J. R., et al. 2017, [Monthly Notices of the Royal Astronomical Society](#), **469**, 1738
- Spergel, D. N., Bean, R., Doré, O., et al. 2007, [The Astrophysical Journal Supplement Series](#), **170**, 377

- Springel, V. 2005, [Monthly Notices of the Royal Astronomical Society](#), 364, 1105
- Tinker, J. L., & et al. in preparation
- Vargas-Magaña, M., Ho, S., Xu, X., et al. 2014, [Monthly Notices of the Royal Astronomical Society](#), 445, 2
- Wang, Q., Sanjeev, K., & Sergio, V. 2009, IEEE TRANSACTIONS ON INFORMATION THEORY, 55, 2392
- Warren, M. S., Abazajian, K., Holz, D. E., & Teodoro, L. 2006, [The Astrophysical Journal](#), 646, 881
- Zhao, C., Kitaura, F.-S., Chuang, C.-H., et al. 2015, [Monthly Notices of the Royal Astronomical Society](#), 451, 4266
- Zheng, Z., Coil, A. L., & Zehavi, I. 2007, [The Astrophysical Journal](#), 667, 760